JOURNAL OF VIROLOGY, Mar. 2010, p. 3033–3042 Vol. 84, No. 6
0022-538X/10/$12.00 doi:10.1128/JVI.01559-09

Measles Virus Infection of Alveolar Macrophages and Dendritic Cells Precedes Spread to Lymphatic Organs in Transgenic Mice Expressing Human Signaling Lymphocytic Activation Molecule (SLAM, CD150)[▽]

Claudia S. Antunes Ferreira,[1]† Marie Frenzke,[1] Vincent H. J. Leonard,[1] G. Grant Welstead,[2] Christopher D. Richardson,[2,3] and Roberto Cattaneo[1]*

Department of Molecular Medicine, and Virology and Gene Therapy Track, Mayo Clinic College of Medicine, Rochester, Minnesota 55905[1]; Department of Medical Biophysics, University of Toronto, and Ontario Cancer Institute, Toronto, Ontario, Canada M5G 2M9[2]; and Department of Microbiology & Immunology/Pediatrics, Dalhousie University Halifax, Nova Scotia, Canada B3H 1X5[3]

Received 28 July 2009/Accepted 21 December 2009

Recent studies of primate models suggest that wild-type measles virus (MV) infects immune cells located in the airways before spreading systemically, but the identity of these cells is unknown. To identify cells supporting primary MV infection, we took advantage of mice expressing the MV receptor human signaling lymphocyte activation molecule (SLAM, CD150) with human-like tissue specificity. We infected these mice intranasally (IN) with a wild-type MV expressing green fluorescent protein. One, two, or three days after inoculation, nasal-associated lymphoid tissue (NALT), the lungs, several lymph nodes (LNs), the spleen, and the thymus were collected and analyzed by microscopy and flow cytometry, and virus isolation was attempted. One day after inoculation, MV replication was documented only in the airways, in about 2.5% of alveolar macrophages (AM) and 0.5% of dendritic cells (DC). These cells expressed human SLAM, and it was observed that MV infection temporarily enhanced SLAM expression. Later, MV infected other immune cell types, including B and T lymphocytes. Virus was isolated from lymphatic tissue as early as 2 days post-IN inoculation; the mediastinal lymph node was an early site of replication and supported high levels of infection. Three days after intraperitoneal inoculation, 1 to 8% of the mediastinal LN cells were infected. Thus, MV infection of alveolar macrophages and subepithelial dendritic cells in the airways precedes infection of lymphocytes in lymphatic organs of mice expressing human SLAM with human-like tissue specificity.

Measles virus (MV), a member of the *Morbillivirus* genus of the *Paramyxoviridae* family, causes measles, a highly contagious disease transmitted by respiratory aerosols that induces a transient but severe immunosuppression (16, 39). In spite of eradication efforts, MV still accounts for about 4% of deaths worldwide in children under 5 years of age (4, 28), due mainly to opportunistic secondary infections facilitated by MV-induced immune suppression (16). Experimental analyses of the mechanisms of pathogenesis, including the characterization of cells and tissues supporting primary MV infection, is limited by host species specificity: old world monkeys and humans are the only natural MV hosts.

MV replication has been characterized mainly around the time of rash appearance, 10 to 14 days after experimental infection of monkeys (8, 9, 26, 46). Viremia in blood cells peaks at or slightly before rash; infected B and T lymphocytes, monocytes, and dendritic cells (DC) are detected, while little if any cell-free virus is produced. Infected cells express the signaling lymphocytic activation molecule (SLAM, CD150), the lymphatic cell MV receptor (13, 20, 47). More information about the cellular targets of wild-type MV infection in the airways immediately after contagion is sought; recent studies of monkeys have suggested that MV may replicate initially in immune cells in the airways (8, 24) rather than in lung epithelial cells as previously postulated (5, 37).

The limited availability and high costs of primate experimentation motivated the development of transgenic rodent models of MV infection. Studies in the ′90s were based on mice expressing human membrane cofactor protein (MCP; CD46), the receptor used only by the attenuated MV strain (11, 31, 55). These studies indicated that airway macrophages are infected by the MV vaccine strain in the first days after intranasal (IN) inoculation and that blood monocytes and tissue macrophages disseminate the infection (29, 36). To increase susceptibility to MV infection, CD46-expressing mice were crossed into an interferon receptor knockout ($Ifnar^{ko}$) background; this did not appear to change the cell-type specificity of viral replication (36).

After human SLAM (hSLAM) was characterized as the immune cell receptor for wild-type and vaccine MV, several mouse strains expressing this protein were generated, as recently reviewed (41). SLAM is a 70-kDa, type I transmembrane glycoprotein expressed on immune cells, such as acti-

* Corresponding author. Mailing address: Mayo Clinic, Department of Molecular Medicine, 200 First Street SW, Rochester, MN 55905. Phone: (507) 538-1188. Fax: (507) 266-2122. E-mail: Cattaneo.Roberto@mayo.edu.

† Present address: Universidade Lusofona de Humanidades e Tecnologias, Avenida do Campo Grande, 376, 1749-024 Lisboa, Portugal.

▽ Published ahead of print on 30 December 2009.

vated T cells, B cells, monocytes/macrophages, and DC (6). It belongs to the immunoglobulin protein superfamily and has two extracellular domains named V and C2; V interacts with the MV attachment protein hemagglutinin (34). SLAM determines Th2 cytokine production, such as that of IL-4, and it may be involved in the production of interleukin 12, tumor necrosis factor alpha, and nitric oxide by macrophages (44, 50, 53). In addition, SLAM may induce B-cell proliferation and immunoglobulin synthesis. Importantly, hSLAM-expressing mice, but not CD46-expressing mice, can be infected by wild-type MV strains that use SLAM but not CD46 as a receptor (32).

Initially a transgenic mouse model expressing hSLAM under the control of the T-cell-specific *lck* promoter was reported (17). In this model, hSLAM expression was restricted to immature and mature lymphocytes in the spleen, thymus, and blood; lymphocyte proliferation was observed, but there were no clinical signs of disease. The second model was a mouse in which the hSLAM coding sequence was expressed under the control of the promoter of the ubiquitously expressed hydroxymethylglutaryl coenzyme A (HMGCoA) reductase protein (40). In suckling mice, generalized but not necessarily relevant infections of most of the major organs were documented. Adult mice were less susceptible to MV infection; only intracerebral inoculation was productive, and it yielded viral proteins but no infectious virus. The third model consisted of a transgenic mouse expressing hSLAM in DC from a cDNA under the control of the CD11c promoter (18). MV infections are limited to DC in this model and disrupt the function of these cells in stimulating adaptive immunity.

An alternative approach to transgenesis seeks human-like tissue specificity of expression. Toward this, Shingai et al. (42) added a full-length hSLAM gene to the mouse genome, showed that indeed these mice express hSLAM with human-like tissue specificity, and crossed them in an Ifnar^{ko} and human CD46-positive background. In this model CD11c-positive DC are instrumental in establishing MV infections. The fifth mouse strain was generated by exchanging only the MV binding site on mouse SLAM with that in the V domain of hSLAM (33). Since humans and mice have similar tissue specificities of SLAM expression, this led to human-like expression. When these mice were crossed in an Ifnar^{ko} background, efficient MV replication suppressing proliferative responses to concanavalin A was documented.

We previously generated a mouse strain expressing hSLAM with human-like tissue specificity in a STAT1-deficient background (54). We showed that hSLAM expression was restricted to B and T lymphocytes and some monocytes/macrophages and that it was inducible by lipopolysaccharide (LPS), lectins, or anti-CD3 antibodies in immune cells, as in primates. Since the Ifnar^{ko} background allows more efficient MV spread (29, 36) without apparent effects on the cell-type specificity of MV infection in mice (33, 42), we crossed here these mice in the Ifnar^{ko} background. We then used the Ifnar^{ko}-SLAMGe mice to identify the cells infected by wild-type MV immediately after IN inoculation. We document efficient early infection of alveolar macrophages (AM) and DC. We also observed subsequent infection of all lymphatic organs and in particular of the mediastinal lymph node (LN), upon both IN and intraperitoneal (IP) inoculation.

MATERIALS AND METHODS

Mouse strains. To establish a transgenic mouse line expressing the hSLAM gene and deficient in the alpha/beta interferon response, Ifnar^{ko}-CD46Ge mice (29) were crossed with SLAMGe mice (54). The hSLAM gene was added to the genome of congenic C57BL/6 mice (54), but the Ifnar^{ko}-CD46Ge mice are on a mixed C57BL/6 and C3H background (29), and the crossing yields a mixed background. To obtain homozygous Ifnar^{ko}-SLAMGe mice, the F_2 and F_3 progeny were screened for inactivation of both copies of the interferon alpha receptor gene (30), for the availability of two copies of the hSLAM gene, and for the absence of the CD46 gene.

Since no simple PCR test for the hSLAM genotype was available, the site of insertion of the hSLAM gene in the mouse genome was characterized. To accomplish this, primers specific for terminal sequences of the human genome inserted in the bacterial artificial chromosome used for transgenesis (54) were synthesized. These primers were used in combination with primers provided in the GenomeWalker universal kit (BD Pharmingen, San Diego, CA) to identify the insertion site of hSLAM in the mouse genome, after nucleotide 47072810 of chromosome 12, in band B3 (mouse genome sequence available through www.ensembl.org). The hSLAM-specific analysis was then based on two combined PCRs. SLAM PCR 1 used the primer pairs 5′-GTGTCACCTAAATAGCTTG GCGTAATCATG and 5′-GTTAATATAGACAATGCCCATCTCCAGCAG, amplifying a 1,030-bp band including part of the hSLAM gene and part of the mouse chromosome 12. SLAM PCR 2 used the primer pairs 5′- AGCTTTCTG AATAGGGGTGTTACTTAATGC and 5′- GTTAATATAGACAATGCCCAT CTCCAGCAG, amplifying a 1,339-bp band of mouse chromosome 12. Mice homozygous for the hSLAM gene had a positive signal from PCR 1 and no signal from PCR 2.

Mouse infections. All animal experimental procedures were performed according to protocols previously approved by the Mayo Clinic Institutional Animal Care and Use Committee. Five- to 8-week-old animals were anesthetized with isoflurane (Novation, IL) and infected IN with 8×10^5 50% tissue culture infectious doses ($TCID_{50}$) of MV in 100 μl divided in two doses of 50 μl (25 μl in each nare) in Opti-MEM. Ten minutes elapsed between both inoculations. Five- to 8-week-old mice were infected IP with 1.5×10^6 $TCID_{50}$ in 1 ml Opti-MEM to measure viral load in lymphatic tissues; for the experiments presented in Table 3, the number of $TCID_{50}$ was 8×10^6. IN and IP infections with 10-fold smaller inocula were productive, but the results were difficult to quantify.

Viruses and virus stock preparation. MVwtIC323 (here abbreviated wtMV) was obtained from an infectious cDNA derived from the Ichinoise B (IC-B) wild-type strain and cloned in the plasmid p(+)MV323 (provided by K. Takeuchi, University of Tsukuba, Tsukuba, Japan) (45). $wtMV_{green}$ is a derivative of MVwtIC323 to which a transcription unit containing the open reading frame of enhanced green fluorescent protein (GFP) (12) was added upstream of the nucleocapsid gene (24). Viruses were amplified on Vero/hSLAM cells as described by Radecke et al. (35). Cells were scraped in Opti-MEM (Gibco/Invitrogen Corp., Grand Island, NY), and viral particles were released by two freeze-thaw cycles. Titers were determined by $TCID_{50}$ titration on Vero/hSLAM cells according to the Spearman-Kärber method (21).

Blood and organ collection and preparation of single-cell suspensions. Blood samples obtained by terminal bleeding by cardiac puncture were collected in a microtainer tube with lithium heparin (Becton Dickinson, Franklin Lakes, NJ). Peripheral blood mononuclear cells (PBMCs) were isolated by density gradient centrifugation with Ficoll-Paque Plus (GE Healthcare, Sweden).

Nasal-associated lymphoid tissue (NALT), LNs, spleens, and lungs were collected aseptically and transferred into a 15-ml tube containing RPMI 1640 (Mediatech Inc., Herndon, VA) with 5% fetal bovine serum (FBS) (Gibco/Invitrogen Corp.) and 1% penicillin/streptomycin (Mediatech Inc.). NALT was collected as follows (1): the facial skin was stripped from the head, and the nose tip, including the front teeth, was cut off. The cheek muscles and cheek bones were taken off. The soft and the hard palate were removed, and the NALT was excised distal to the emergence of the palatine nerve. To obtain single-cell suspensions, NALT, LNs, and spleens were transferred to a 70-μm-pore-size cell strainer (BD Biosciences, Bedford, MA), mashed with the plunger of a syringe, washed with RPMI 1640 medium, and resuspended in this medium.

Single-cell suspensions from lungs were generated as described in reference 38, with some modifications. Briefly, the lungs were aseptically collected in 10 ml of RPMI 1640 with 5% FBS and 1% penicillin/streptomycin, reduced to small pieces (approximately 1 to 2 mm^2), and digested at 37°C for 1 h in 10 ml phosphate-buffered saline (PBS) (Mediatech) containing 300 U/ml collagenase type II (Worthington, Lakewood, NJ) and 0.15 mg/ml DNase (Roche Diagnostics, Germany). After digestion, lung pieces were minced with the plunger of a

syringe and washed in a 70-μm-pore-size cell strainer with RPMI 1640. Cells were centrifuged and resuspended in 3 ml of red cell lysis buffer (ACK lysis buffer; 0.15 M NH_4Cl, 1 mM $KHCO_3$, 0.1 mM EDTA, pH 7.2) and incubated at 37°C for 3 min. Cell suspensions were washed once with RPMI 1640 medium in a 70-μm-pore-size cell strainer, centrifuged, and resuspended in RPMI 1640 medium.

Immunohistochemistry and immunofluorescence. Initial preparation of tissues was as follows: tissues were collected at different time points after infection, embedded in Tissue-Tek OCT compound (Sakura Finetek, Torrence, CA), and frozen by immersion in liquid nitrogen-cooled methylbutane (Sigma-Aldrich Inc., St. Louis, MO). Tissue sections 4 to 6 μm in thickness were obtained, fixed in 99.5% histological-grade acetone (Sigma-Aldrich), and stored at −80°C until further use. Sections were thawed at room temperature (RT) for 5 min and fixed in 2% paraformaldehyde solution (USB Corporation, Cleveland, OH) for 10 min.

For immunohistochemistry staining, frozen sections were incubated with peroxidase blocking reagent (Dako, Carpinteria, CA) for 30 min at RT, incubated with background reducer solution (Background Sniper, Biocare Medical, Concord, CA) for 30 min at RT, and incubated with anti-MV N polyclonal antibody (48) diluted in Background Sniper solution for 1 h at RT. Sections were then washed with Bio-Rad Tris-buffered saline (20 mM Tris, 500 mM NaCl) and incubated with rabbit or rodent alkaline phosphatase-polymer solution (Biocare Medical) for 20 min at RT. Alkaline phosphatase was visualized with red chromogen substrate (Biocare Medical). Sections were counterstained with hematoxylin (Vector, Burlingame, CA) and mounted with permanent mounting medium (Vector).

For immunofluorescence staining, sections were permeabilized for 3 min at RT in PBS with 0.1% (vol/vol) Triton X-100 (Sigma-Aldrich). Sections were incubated with 5% goat serum blocking solution for 30 min at RT. Streptavidin-biotin blocking was performed prior to incubation of sections with biotinylated anti-major histocompatibility complex class II (MHC-II) (I-A^b) antibody, using a streptavidin-biotin blocking kit (Vector). After blocking, sections were incubated 1 h at RT with antibodies diluted, according to the manufacturer's recommendations, in blocking solution. MV N protein was detected with a rabbit polyclonal anti-MV N antibody (described above) at a dilution of 1:100 and incubated with Alexa Fluor 488-conjugated anti-rabbit IgG (Molecular Probes; Invitrogen, Eugene, OR). B lymphocytes were identified with anti-CD45 (B220) (clone RA3-6B2; BD Biosciences Pharmingen); CD4 and CD8 T cells were identified with anti-CD4 (YTS191.2; Abcam Inc., Cambridge, MA) and anti-CD8 (YTS169.4; Abcam), respectively; AM were characterized with anti-CD2 (LFA-2) (RM2-5; eBioscience, San Diego, CA), anti-CD11c (223H7; MBL International, Woburn, MA), anti-F4/80 (Cl:A3-1; Abcam), biotinylated mouse monoclonal anti-MHC-II (I-A^b) (AF6-120.1; BD Pharmingen), and anti-Mac-1 (M1/70; eBioscience). Epithelial cells were identified with anti-CD326 (epithelial cell adhesion molecule [Ep-CAM]) (G8.8, BD Biosciences Pharmingen). Secondary antibodies included Alexa Fluor 594-conjugated anti-rat IgG (Invitrogen). Sections stained with biotinylated mouse monoclonal anti-MHC-II (I-A^b) as primary antibody were stained with Alexa 594-conjugated streptavidin (Invitrogen) as the secondary antibody. Sections were mounted in Prolong Gold antifade reagent with DAPI (4′,6-diamidino-2-phenylindole) (Invitrogen; Molecular Probes) and visualized with a Zeiss Axioplan confocal microscope (LSM 510; Carl Zeiss Inc., Germany).

Flow cytometry. For flow cytometry analysis, whole lungs were collected without lavage, to allow the inclusion of bronchoalveolar cells. A single-cell suspension was prepared as described above. Cells were counted using a hemacytometer after diluting with trypan blue dye to exclude dead cells. Isolated cells were resuspended at a density of 10^6 cells/50 μl. To identify specific cell subpopulations, a multicolor staining was performed by incubating cells with appropriate antibodies (1 μg per million cells), for 45 min on ice. GFP was assessed to identify MV-infected cells. For the identification of $CD4^+$ T cells, anti-CD4-phycoerythrin (PE) (H129.19; BD Pharmingen) and anti-CD3-allophycocyanin (APC)-Cy7 (17A2; eBioscience) antibodies were used. For the identification of $CD8^+$ T cells, cells were stained with anti-CD8-PE-Cy7 (53-6.7; eBioscience) and anti-CD3-APC-Cy7 (eBioscience) antibodies. B lymphocytes were identified with anti-CD45R (B220)-APC-Cy7 (RA3-6B2; eBioscience). In order to reduce Fc receptor binding, cells stained with CD45R (B220) antibody (B cells) were first incubated with CD16/32 antibody (2.4G2; BD Pharmingen) for 5 min on ice. DC (conventional) were identified with anti-MHC-II (I-A^b)-PE (AF6-120.1; BD Pharmingen) and anti-CD11c-APC (HL3; BD Pharmingen). Macrophages were stained with anti-CD11c-APC (HL3; BD Pharmingen) and anti-Mac-1-PE-Cy5 (M1/70; eBioscience). AM were identified with the following staining: anti-Mac-1-PE-Cy5 (M1/70; eBioscience), anti-F4/80-APC-Cy7 (BM8; eBioscience), anti-CD11c-APC (HL3; BD Pharmingen), and anti-MHC-II (I-A^b)-PE (AF6-120.1; BD Pharmingen). Epithelial cells were identified with anti-CD326-PE (Ep-CAM) (G8.8; BD Pharmingen). $Ifnar^{ko}$-CD46Ge mice were used as negative controls for quantification.

Human SLAM expression was detected by incubating cells with biotin anti-human CD150 [A12 (7D4); BioLegend, San Diego, CA] and then incubating them with streptavidin-PerCP (Becton Dickinson Immunocytometry Systems, San Jose, CA). $Ifnar^{ko}$-CD46Ge mice were used as negative controls, and mock-infected animals were used as a negative control for GFP expression. Acquisition of samples was performed on a cytometer (FacsCanto or LSRII; BD Biosciences) and analyzed using FlowJo software (Tree Star Inc., Asland, OR). Statistical analysis was performed with standard paired *t* tests using the JMP7 software (SAS, Cary, NC).

Quantification of virus load in lymphatic organs. Single-cell suspensions from mandibular, mediastinal, mesenteric, and inguinal LNs and spleens were obtained as described above. Serial 10-fold dilutions of mononuclear cells were made in DMEM with 5% FBS and 1% penicillin/streptomycin. Four replicates of 10^1 to 10^5 mononuclear cells were cocultured with 5×10^5 Vero/hSLAM cells in 24-well plates, and 10^6 mononuclear cells were cocultured with 10^6 Vero/hSLAM cells in a 100-mm dish. Cultures were monitored for cytopathic effects 4 days later. Virus titers were expressed as $TCID_{50}$ per 10^6 cells.

RESULTS

$Ifnar^{ko}$-SLAMGe transgenic mice. To generate mice susceptible to wild-type MV infection, the hSLAM gene, including all its transcription control elements, was previously transferred to the mouse genome (54). In another approach to enhance replication of any exogenous virus in mice (30), the mouse interferon type I receptor gene was inactivated ($Ifnar^{ko}$ background). For our study we combined these desirable characteristics by crossing hSLAM-expressing with $Ifnar^{ko}$ mice; to facilitate progeny screening, we mapped the insertion site of the hSLAM gene in the mouse genome, as detailed in Materials and Methods. The resulting mouse strain was named $Ifnar^{ko}$-SLAMGe. It is defective in the interferon type I response and expresses hSLAM with human-like tissue specificity; for example, 11 to 13% CD3-positive T cells of these mice express hSLAM (data not shown), compared to 10 to 20% CD3-positive T cells of humans (6, 43); 28 to 31% CD19-positive B cells of these mice express hSLAM, compared to 20 to 25% CD20-positive B cells of humans (data not shown).

hSLAM expression in lymphatic tissue of $Ifnar^{ko}$-SLAMGe transgenic mice. We document here cell-type specificity of hSLAM expression in the mediastinal LN, previously shown to be important for MV infection of SLAM "knock-in" mice (33); in these mice, MV reaches higher titers in this LN than in other lymphatic organs. Single-cell suspensions were prepared from the mediastinal LNs of five uninfected $Ifnar^{ko}$-SLAMGe mice and stained with specific markers to indentify B cells (B220), T cells (CD3), and macrophages ($CD11c^{low}$ $Mac\text{-}1^{high}$). Cells were gated for live leukocytes and analyzed for hSLAM expression within each cell population.

Figure 1 documents hSLAM expression in one representative animal. About 5% B cells (Fig. 1A, left, compare top left and right quadrants) and 2% T cells (Fig. 1B, left, compare top left and right quadrants) scored positively; the right panels in Fig. 1A and B document hSLAM expression levels in $Ifnar^{ko}$-SLAMGe mice (red line) compared to a negative control ($Ifnar^{ko}$-CD46Ge mice, blue line). The mean and standard deviation of SLAM expression in the mediastinal LNs of five animals were 10 ± 5.9% for B cells and 1.5 ± 0.6% for T cells (data not shown). Thus, resting B and T cells from the mediastinal LNs of $Ifnar^{ko}$-SLAMGe mice express hSLAM at low

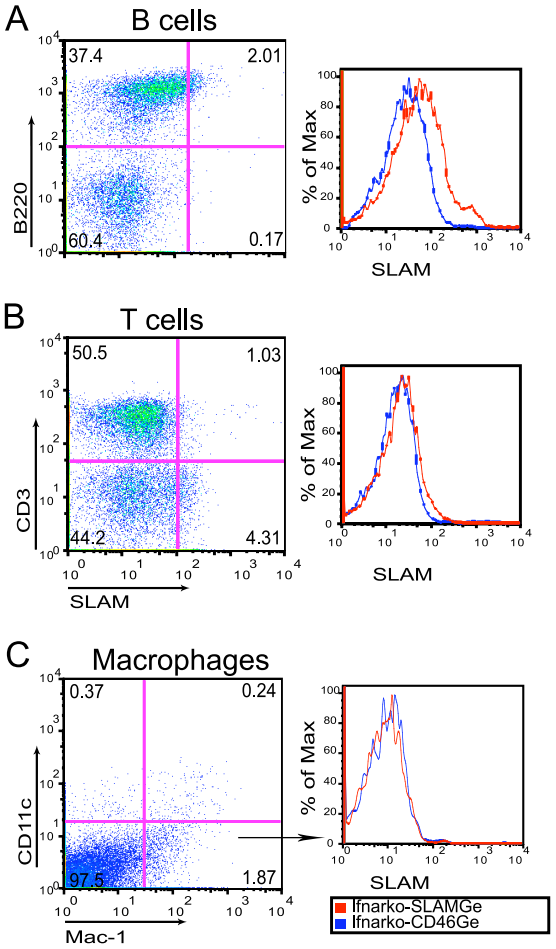

FIG. 1. Analysis of hSLAM expression in leukocytes from the mediastinal LNs of Ifnar^{ko}-SLAMGe mice. Cells were stained with antibodies specific for B cells (B220^{+}) (A), T cells (CD3^{+}) (B), or macrophages (CD11c^{low} Mac-1^{high}) (C). Ifnar^{ko}-CD46Ge mice were used as negative controls (right, blue lines). % of Max is a measure of the number of cells normalized to the same total number in each sample.

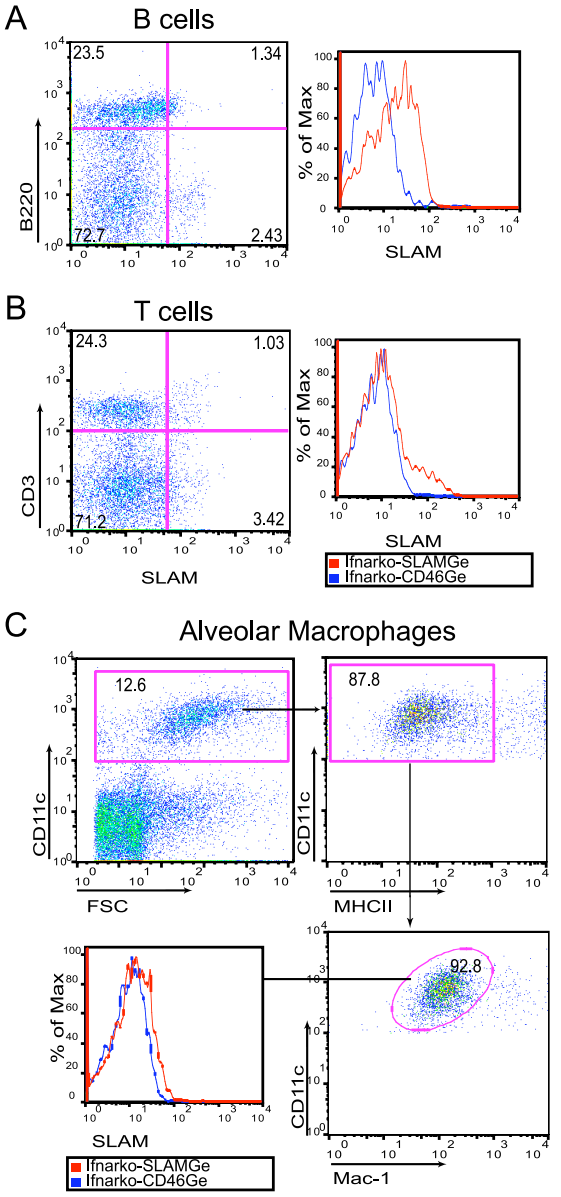

FIG. 2. Analysis of SLAM expression in leukocytes from the lungs of Ifnar^{ko}-SLAMGe mice. (A and B) Lymphocytes were gated and sorted with antibodies against B cells (B220^{+}) or T cells (CD3^{+}), respectively. For AM (C), total live cells were stained with three antibodies and sorted for the combination CD11c^{high} MHCII^{low} Mac-1^{low}. Ifnar^{ko}-CD46Ge mice were used as negative controls. For histograms, % of Max is a measure of the number of cells normalized to the same total number in each sample. FSC, forward scatter.

levels, and more B than T cells express this protein, as in human lymphatic tissues (2, 7). In CD11c^{low} Mac-1^{high} macrophages of this mouse (Fig. 1C, left, bottom right quadrant), hSLAM expression was below the detection level (Fig. 1C, right).

Human SLAM expression in immune cells of the lungs of Ifnar^{ko}-SLAMGe transgenic mice. Since primary wtMV replication occurs mainly if not exclusively in immune cells, rather than in epithelial cells (24), SLAM-expressing immune cells in the airways or in subepithelial tissue are candidate hosts for virus replication. We thus characterized hSLAM expression in single-cell suspensions obtained from lungs of uninfected Ifnar^{ko}-SLAMGe mice, including B cells (B220^{+}), T cells (CD3^{+}), and AM defined as CD11c^{high} MHCII^{low} Mac-1^{low} F4/80^{high} cells (14, 22).

Figure 2 documents hSLAM expression in these cells. About 5% of B cells (Fig. 2A, left, compare top left and right quadrants) and 4% of T cells (Fig. 2B, left, compare top left and right quadrants) of one animal scored positively; the right panels in Fig. 2A and B document hSLAM expression levels in Ifnar^{ko}-SLAMGe mice (red line) compared to a negative control (Ifnar^{ko}-CD46Ge mice, blue line). The mean and standard deviation of SLAM expression in lung tissue of five animals were 8.7 ± 1.9% for B cells and 3.3 ± 0.7% for T cells (data not shown). A small fraction of AM also express SLAM (Fig. 2C, lower left, compare red line of Ifnar^{ko}-SLAMGe mice with blue line of Ifnar^{ko}-CD46Ge negative control mice).

Early wtMV replication in the lungs of Ifnar^{ko}-SLAMGe transgenic mice. We then sought to identify the tissue and cell types sustaining wtMV replication immediately after IN inoc-

TABLE 1. MV reisolation from organs of Ifnar^{ko}-SLAMGe mice after IN infection

Organs	No. positive/total no.			
	Day 1[a]	Day 2	Day 3	Day 7
Lungs	5/5	3/3	3/3	3/3
NALT	0/5	0/3	0/3	0/3
Mandibular LN	0/5	0/3	1/3	2/3
Mediastinal LN	0/5	2/3	3/3	3/3
Thymus	0/5	ND[b]	0/3	2/3
Spleen	0/5	0/3	3/3	2/3
PBMC	0/5	0/3	1/3	1/3

[a] Day p.i.
[b] ND, not done.

ulation of Ifnar^{ko}-SLAMGe mice. Candidate host tissues/cell types include NALT and immune cells in the airway lumen or subepithelial airway tissue. Mice were inoculated with wtMV$_{green}$, a GFP-expressing virus; since wtMV interacts with SLAM but not CD46, Ifnar^{ko} mice expressing CD46 but not SLAM served as a negative control. One to seven days after IN inoculation, as indicated in Table 1, NALT and the lungs were harvested; in addition, mandibular and mediastinal LNs, thymuses, spleens, and PBMC were collected. Cells from these organs were cocultured with Vero/hSLAM cells, and the appearance of syncytia was monitored over 4 days.

As shown in Table 1, wtMV was isolated from the lungs of every Ifnar^{ko}-SLAMGe mouse at every time point. Virus was also isolated from the lungs of all three Ifnar^{ko}-CD46Ge mice sacrificed 1 day postinfection (p.i.), but not at later time points (data not shown), suggesting that some of the virus reisolated at day 1 may be the inoculum. At 2 days p.i., virus was recovered from the mediastinal LNs in 2 out of 3 animals. At 3 and 7 days p.i., virus was isolated from the mediastinal LN and the spleen of most mice and from the mandibular LN, thymus, and PBMC of some mice. However, no virus was isolated from the NALT of any animal. These observations suggest that wtMV replicates initially in the lungs of Ifnar^{ko}-SLAMGe mice and then spreads to lymphatic organs through infected cells circulating in the lymphatics rather than in the blood.

To assess whether the inoculum accounts for a significant fraction of the signal detected after inoculation, we infected Ifnar^{ko}-SLAMGe mice IN with UV-inactivated wtMV$_{green}$. Mice were sacrificed 1, 2, or 3 days after inoculation, and whole lungs examined under a fluorescence microscope; no fluorescence was detected in mice infected with UV-inactivated virus. On the other hand, the pattern of GFP expression was quite homogeneous; in four of four Ifnar^{ko}-SLAMGe mice inoculated with live virus, green fluorescence was observed with all the lobes of the lung and reached into the lower respiratory airways (data not shown). As an additional control, we infected Ifnar^{ko}-CD46Ge mice with wtMV$_{green}$, but again no fluorescence was detected with the lungs of these animals (data not shown). Since the UV-inactivated inoculum is not detectable by analysis of GFP fluorescence, we conclude that 1 day postinoculation significant MV replication accounts for strong GFP expression.

AM sustain wtMV replication in the lungs. We then assessed by immunohistochemistry (Fig. 3A and B) and immunofluorescence (Fig. 3C to H) which cell types sustain MV replication in the airways. Ifnar^{ko}-SLAMGe mice were infected IN with wtMV$_{green}$, and lungs were collected 1 day postinoculation, frozen, and stained with an anti-N antibody (red). Figure 3A and B show one representative immunohis-

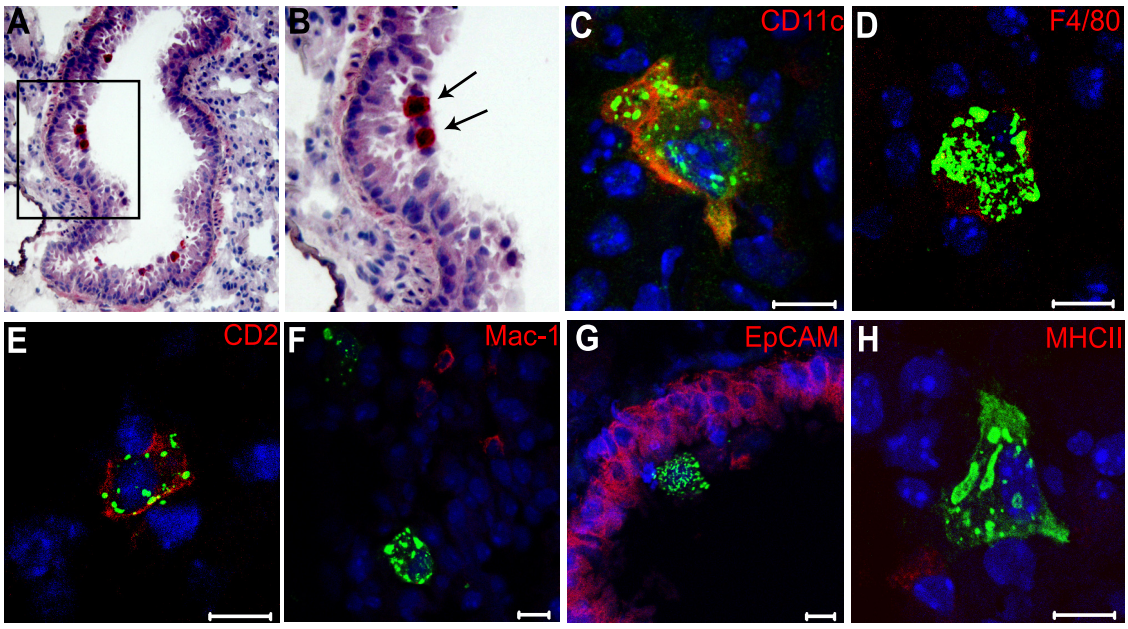

FIG. 3. Characterization of wtMV-infected cells in the lungs 1 day after mouse inoculation. (A and B) Frozen sections of mouse lung stained with an anti-N antibody and counterstained with hematoxylin. N protein was visualized with red chromogen. Arrows indicate positive cells, which localize in the airway lumen. (C to H) Identification of the cell types accumulating MV N by confocal micrograph analysis of lung frozen sections. N protein was visualized with Alexa Fluor 488 (green). The specific cell markers indicated on the top right of each panel were visualized with Alexa Fluor 594 (red). Nuclei were counterstained in blue with DAPI. Scale bars represent 10 μm.

TABLE 2. Percentile of wtMV-infected cells in the lungs 1 and 3 days after IN inoculation[b]

Cell type[a]	Day 1 (6 mice)	Day 3 (10 mice)	Mock (5 mice)
B cells ($B220^+$)	0.3 ± 0.1 (8–64)	0.1 ± 0.1 (1–20)	0
$CD4^+$ T cells ($CD3^+$ $CD4^+$)	0.2 ± 0.1 (1–7)	0.7 ± 0.8 (0–52)	0.01 ± 0.02 (0–1)
$CD8^+$ T cells ($CD3^+$ $CD8^+$)	0.1 ± 0.04 (1–3)	0.1 ± 0.1 (0–3)	0
DC ($MHCII^{high}$ $CD11c^{high}$)	0.5 ± 0.2 (5–11)	0.3 ± 0.2 (0–4)	0.1 ± 0.2 (0–2)
AM ($CD11c^{high}$ $MHCII^{low}$ Mac-1^{low} F4/80^{high})	2.4 ± 0.9 (90–330)	0.7 ± 0.4 (9–77)	0
Monocytes (Mac-1^{high} $CD11c^{low}$)	0	0.4 ± 0.2 (2–10)	0
Epithelial cells ($EpCAM^+$)	0.1 ± 0.02 (4–13)	0.1 ± 0.1 (1–10)	0.04 ± 0.02 (2–4)

[a] Number of cells counted were over 5,000 B cells, AM, and epithelial cells; about 3,000 $CD4^+$ and $CD8^+$ T cells; about 1,500 monocytes; and about 1,200 DC.
[b] Values are average ± standard deviation (range of counts).

tochemistry analysis; MV N protein was most often detected with cells located on the luminal side of respiratory bronchioles, a location typical for AM.

To assess the identity of infected cells and differentiate between AM and other immune cells, including DCs, we stained lung sections with an anti-N antibody (green) and different cellular markers: the immune cells markers CD11c, F4/80, CD2 (also named LFA-2), Mac-1 (also named CD11b) and MHC-II, and the epithelial cell marker EpCAM (14, 22). None of the infected cells were EpCAM positive (Fig. 3G), suggesting that epithelial cells are not infected. Infected cells were often CD11c, F4/80, and CD2 positive (Fig. 3C to E) but very rarely Mac-1 or MHC-II positive (Fig. 3F and H). Even if none of the above markers is entirely specific for one type of immune cells, all together, these results suggest that AM may sustain primary wtMV infection in the lungs.

To quantify the level of infection of AM and other immune cell types, mice inoculated IN with $wtMV_{green}$ were sacrificed 1 or 3 days later. Lungs were collected, tissue cells were dissociated, and GFP expression was analyzed using flow cytometry. The analysis presented in Table 2 indicates that AM (sorted as $CD11c^{high}$ $MHCII^{low}$ Mac-1^{low} F4/80^{high} cells) were infected at the highest levels (2.4 ± 0.9%) 1 day postinoculation ($P = 0.0016$ between AM and epithelial cells). Conventional DC (sorted as $MHCII^{high}$ $CD11c^{high}$ cells) were infected at about five times lower levels (0.5 ± 0.2%; $P = 0.0024$ between DC and epithelial cells), whereas only 0.1 to 0.3% of different populations of lymphocytes were infected. Near-background (0.1%) levels of infection of epithelial cells were documented.

At day 3 postinfection low (0.1 to 0.7%) levels of infections were documented for all immune cell types analyzed, with AM and CD4 T cells being infected at the highest levels; monocytes that are available in unperfused lungs were infected at levels similar to those of other immune cell types (0.4%). Epithelial cell infection remained near background (0.1%). These data confirm that AM are the main initial target cells for wtMV infection and also indicate that wtMV replication in immune cells located in the mouse airways is limited and short lived. We also detected cellular infiltrates in the lungs 3 days p.i., which was due mainly to neutrophils (data not shown).

wtMV infects AM expressing SLAM, and MV infection enhances SLAM expression. To assess whether hSLAM expression correlates with MV infection, we inoculated $Ifnar^{ko}$-SLAMGe mice IN with $wtMV_{green}$ and analyzed hSLAM expression on AM collected 1 day after inoculation. AM from mock-infected $Ifnar^{ko}$-SLAMGe mice and from infected $Ifnar^{ko}$-CD46Ge mice served as controls. AM were sorted as $CD11c^{high}$, $MHCII^{low}$, and Mac-1^{low} cells (Fig. 4).

Figure 4A (far right, right quadrants) shows that background (0.12%) SLAM expression was detected with AM from control $Ifnar^{ko}$-CD46Ge mice. On the other hand, 0.86% of AM of $Ifnar^{ko}$-SLAMGe mice mock infected with the postnuclear fraction of uninfected Vero/hSLAM cells expressed SLAM (Fig. 4B, far right, right quadrants). Remarkably, about 16% (1.44% GFP-positive and 14.8% GFP-negative) of AM of infected $Ifnar^{ko}$-SLAMGe mice expressed SLAM (Fig. 4C, far right), which may reflect AM activation.

Importantly, about 1 in 11 SLAM-expressing AM were infected (Fig. 4C, compare numbers in top and bottom right panels), whereas 1 in 28 SLAM-negative AM were infected (Fig. 4C, compare numbers in top and bottom left panels). Analysis of AM from an additional four animals confirmed two or three times preferential infection of SLAM-expressing cells (data not shown). These data confirm that infection of AM in a SLAM-dependent manner is a crucial step in the early stages of MV infection. Enhanced hSLAM expression on infected and noninfected AM is short lived: 3 days after infection, hSLAM expression returned to levels slightly above the values found on AM from mock-infected mice (data not shown).

Spread in the lymphatic organs. We further characterized wtMV spread by quantifying viral replication in different lymphatic organs of $Ifnar^{ko}$-SLAMGe mice 3 days after IN inoculation. As shown in Fig. 5A, the mediastinal LNs were infected with high efficiency in two mice and at lower levels in three other animals, whereas the other lymphatic tissues (mandibular, mesenteric, and inguinal LNs and spleens) were infected at low or undetectable levels. Thus, the mediastinal LN that drains the respiratory tract appears to be a prominent site of wtMV replication after IN infection of $Ifnar^{ko}$-SLAMGe mice, as well as knock-in hSLAM-expressing mice (33).

We then asked whether this effect is due to the IN route of infection or to a stronger susceptibility of cells in the mediastinal LN to wtMV infection. We inoculated mice IP and compared replication levels in a LN located in the peritoneum (mesenteric), one in the thoracic cavity (mediastinal), and two control lymph nodes (mandibular and inguinal). Three days later lymphatic tissues were harvested, and the viral load was measured. Again, a high wtMV titer was documented for the mediastinal LN (Fig. 5B): in different mice 1 to 8% of the cells of this LN were infected 3 days p.i. The average levels of infected cells in the mandibular, mesenteric, and inguinal LNs and the spleens were 10 to 100 times lower, but the differences between different LNs were not statistically significant. Six days

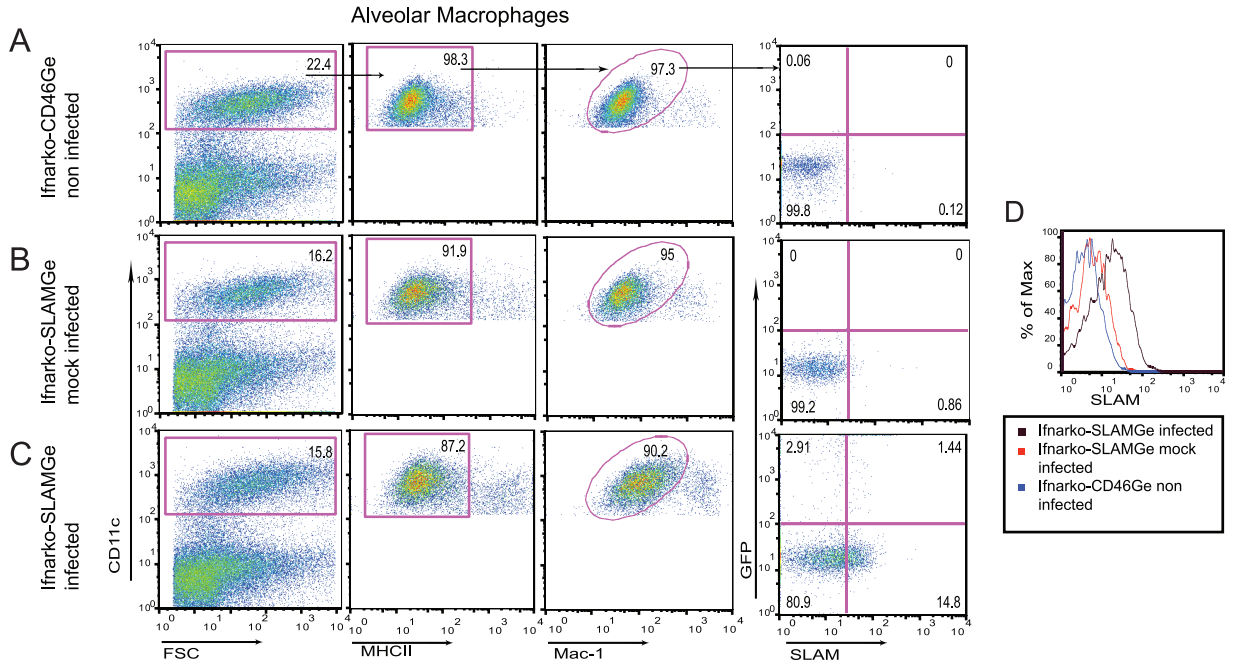

FIG. 4. Analysis of hSLAM expression in AM before and after wtMV infection. AM from noninfected Ifnar^{ko}-CD46Ge mice (A), mock-infected Ifnar^{ko}-SLAMGe (B), or MV-infected Ifnar^{ko}-SLAMGe mice (C). Cells were gated for CD11c^{high} (left), MHCII^{low} (center left), and Mac-1^{low} (center right) and analyzed for infection (GFP) versus SLAM expression (right). Effect of MV infection on hSLAM expression in AM (D). FSC, forward scatter. Ifnar^{ko}-CD46Ge mice were used as negative controls to set the quadrants.

p.i. (Fig. 5C), 0.01 to 0.1% of the cells were infected in all lymph nodes and in the spleen.

Finally, we sought to identify which cells support wtMV replication in the mediastinal LN and whether infection correlates with SLAM expression. A group of 6 Ifnar^{ko}-SLAMGe mice was inoculated IP, mediastinal LNs were collected 3 days p.i., single-cell suspensions were obtained, and GFP expression was analyzed by flow cytometry. As shown in Table 3, lymphocytes were infected at the highest levels: 2 ± 0.7% of B cells (B220$^+$), 1.1 ± 0.3% of CD4$^+$ T cells (CD3$^+$ CD4$^+$), and 2 ± 0.4% of CD8$^+$ T cells (CD3$^+$ CD8$^+$). DC (MHCII^{high} CD11c^{high}) were infected at similar levels (1.4 ± 0.4% infection), but macrophages (CD11c^{low} Mac-1^{high} MHCII^{high}) were infected at lower levels (0.6 ± 0.1%). We note that DC and macrophages account only for a small fraction of cells in the mediastinal LN and thus that lymphocytes are by far the most abundant cell type infected.

DISCUSSION

A new small-animal model of MV infection. Small-animal models for measles do not mimic exactly the human disease but allow one to focus on particular aspects of infection. We focused our study on the question of which cells are infected immediately after respiratory inoculation and documented that hSLAM-expressing AM, as well as DC, are the initial targets in the lungs. These cells may ferry the infection through the epithelial barrier. Similarly, recent work with wild-type and selectively receptor-blind MVs (8, 24) and with a selectively receptor-blind canine distemper virus (52) provided evidence for a model of morbillivirus dissemination postulating that these viruses take advantage of SLAM-expressing immune cells situated in the lumen of the respiratory tract of natural hosts to cross the epithelial barrier after contagion.

Our improved mouse model has an immune-deficient background: we generated hSLAM transgenic mice whose innate immune systems are compromised by the deletion of the interferon alpha receptor. As expected, the Ifnar^{ko} background allowed more extensive MV infections than the previously used STAT1-defective background (54). Minimal MV replication in hSLAM-expressing mice that are immunocompetent did not allow a sensitive study of the cell-type specificity of infection, and we do not know whether prevention of the interferon type I response induces a different cell-type specificity of infection. However, we know this was not the case for other mouse strains expressing CD46 or hSLAM in Ifnar^{ko}-background mice (33, 42), and we do not have indications of the contrary for our mouse strain.

Most characteristics of the Ifnar^{ko} and the STAT1-defective strain were similar. For example, equivalent levels of SLAM expression were observed with different cell types. Moreover, for the STAT1-defective mice, we reported enlarged lymph nodes and splenomegaly due to immune cell infiltration (54); similarly, 6 days postinoculation we observed enlarged lymph nodes with the Ifnar^{ko} mice, and the weight of their spleens was on average double the normal amount (119.8 ± 23.4 mg versus 54.8 ± 6.2 mg in uninfected mice [average and standard deviation in groups of five mice]).

The cell-type specificity of expression of hSLAM suggests that a wild-type MV might infect certain target lymphocytes, monocytes/macrophages, and DC in transgenic mice. Indeed, we monitored and quantified MV entry in these cell types and documented predominant interactions with AM and DC 1 day

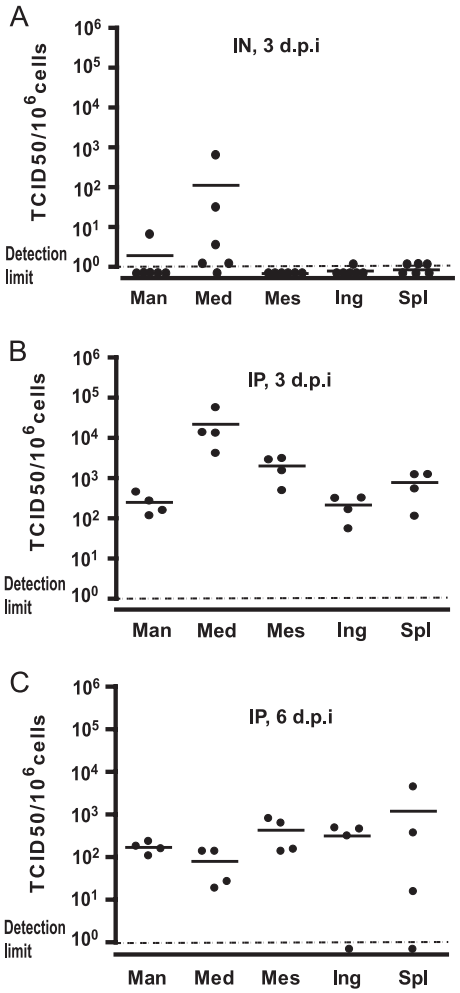

FIG. 5. wtMV infection levels in lymphatic organs. Data were obtained 3 days after IN inoculation (A), 3 days after IP inoculation (B), or 6 days after IP inoculation (C). Each dot represents a single mouse. Group average is represented by a horizontal bar, and detection limit by a dotted line. Man, mandibular LN; Med, mediastinal LN; Mes, mesenteric LN; Ing, inguinal LN; Spl, spleen.

after IN inoculation. To our knowledge, this report is the first direct analysis of the events that support primary MV replication and early viral spread in an animal model. Later, infection progresses to lymphatic tissues, with an early (2 days p.i.) involvement of the mediastinal LN. Lymphocytes sustain the bulk of MV infection not only in the mediastinal LN (Table 3) but also in other LNs and lymphatic organs (data not shown). Thus, our model reproduces the lymphatic phases of the infections of MV and other morbilliviruses in their natural hosts (26, 51).

Crossing the epithelial barrier: alternatives. One day after IN inoculation with 10^6 $TCID_{50}$, MV replication was documented for about 2.5% of AM and 0.5% of DC of hSLAM-expressing mice. MV replication was below detection levels in $Ifnar^{ko}$ mice not expressing hSLAM, indicating that scavenging of infectious virus by $Ifnar^{ko}$ AM rarely if at all results in productive infection. Since there are about 2 million AM in a mouse (49), about 5×10^4 AM were productively infected and expressed GFP. Even if only 1 in 1,000 infected AM crosses the lung epithelium, about 50 of these cells would have the opportunity to transmit infectivity to the lymphatic organs. AM are implicated in the translocation of particles from the lungs to the draining lymph nodes (19), a process that MV may exploit to cross the epithelial barrier: infected AM might migrate to the draining lymph nodes and spread infection to B and T lymphocytes. The fact that replication of an MV vaccine strain in CD46-expressing transgenic mice is most prominent for macrophages after inoculation by three different routes (36) is consistent with these cells sustaining the immediate-early phase of MV infection. Moreover, for $Ifnar^{ko}$-CD46Ge mice, *in vivo* depletion of AM resulted in strong local DC infiltration, virus infection of infiltrating DCs and macrophages, and ultimately higher virus titers for lymphatic tissues (36). Thus, while protecting other immune cells from infection, AM also support MV replication in the lungs and are likely to be one of the pathways exploited by MV to cross the epithelial barrier.

Another potential ferry for MV are DC present in the subepithelial tissues of the airways. We have observed that there are about 10 times less DC than AM in the lungs of mice and estimate that about 0.5% of 2×10^5 DC, or about 1,000 DC, are infected. It has been reported that DC infected with influenza virus rapidly migrate from the respiratory tract to the draining LN (15), beginning 2 h after infection (23). Analogously, DC productively infected with MV might cross the epithelial barrier and rapidly disseminate virus in the lymphatic organs, including the mediastinal LN. Alternatively, the virus would attach to DC through DC-SIGN but not replicate, and DC would transinfect T lymphocytes (10). DC that carry low levels of MV may be detected inefficiently by flow cytometry, resulting in an underestimation of the efficiency of infection. Finally, it is also possible that cell-free virus exploits breaks in the epithelial barrier to reach immune organs through the lymphatics, but the efficiency of AM and DC infection is consistent with either cell type being more important than epithelium leakage as the primary means for MV to cross the epithelial barrier.

SLAM expression and virus amplification. Ohno et al. (33) observed that the mediastinal LN is preferentially infected in mice expressing a human-mouse SLAM hybrid, and several lines of evidence in our study suggest that a similar phenomenon occurs in our mice expressing hSLAM. To assess whether this is explained simply by higher receptor expression, we measured hSLAM expression levels in this and the mesenteric, mandibular, and inguinal LNs of uninfected animals but failed to document significant differences (data not shown). Thus, the

TABLE 3. Percentile of infected cells in the mediastinal LN after IP inoculation[a]

Cell type	Day 3	Mock
B cells ($B220^+$)	2 ± 0.7 (362–851)	<0.01 (0–1)
$CD4^+$ T cells ($CD3^+$ $CD4^+$)	1.1 ± 0.3 (159–332)	<0.01 (0–1)
$CD8^+$ T cells ($CD3^+$ $CD8^+$)	2 ± 0.4 (188–313)	0.02 ± 0.01 (1–5)
DC ($MHCII^{high}$ $CD11c^{high}$ Mac-1^{low})	1.4 ± 0.4 (18–54)	0.08 (0–2)
Macrophages ($CD11c^{low}$ Mac-1^{high})	0.6 ± 0.1 (10–22)	0.01 (0–2)

[a] Average ± standard deviation (range of counts); group size was 6 animals (both groups).

cause for preferential MV spread in the mediastinal LN remains to be determined.

In transgenic mice (Fig. 4), as in human tonsillar tissue (7), MV infects predominantly, but not exclusively, immune cells expressing SLAM. We do not know if the apparently SLAM-independent entry really occurs; it is possible that hSLAM expression is undetectable with antibodies but still sufficient to facilitate viral entry.

After IN inoculation with MV, hSLAM expression is enhanced in infected and noninfected AM. Similarly, *ex vivo* induction of SLAM expression after MV infection was previously reported for monocytes (3, 27). The mechanisms activating SLAM expression in both systems are unknown and could be indirect. Nevertheless, since SLAM is a low-affinity self-ligand glycoprotein (25), increase of its expression in few target cells may cause a feedback loop of cell activation. This feedback loop may in turn sustain extremely rapid spread of *Morbillivirus* infections in natural hosts (51).

The new mouse model developed in this study allowed characterization of the immediate-early phases of wild-type MV infection in the respiratory airways of an interferon-defective host and gave quantitative insights in the cell types supporting primary MV replication in the lungs of this host. Future studies will address the relative importance of AM and DC for supporting primary MV infection and ferrying virus through the epithelial barrier in mice and the question of the levels of infection of these cells in interferon-competent hosts.

ACKNOWLEDGMENTS

We thank C. Springfeld for designing the PCR assay for the hSLAM gene and K. C. Yaiw, J. Reyes del Valle, and P. Devaux for helpful suggestions and discussions and for comments on the manuscript. We thank M. Bennett for excellent secretarial assistance.

This work was supported by a grant from the National Institutes of Health (CA90636 to R.C.), by a predoctoral fellowship to C.S.A.F. from the Fundacao para a Ciencia e Tecnologia of Portugal, and by the Mayo Foundation for Medical Education and Research.

REFERENCES

1. **Asanuma, H., A. H. Thompson, T. Iwasaki, Y. Sato, Y. Inaba, C. Aizawa, T. Kurata, and S. Tamura.** 1997. Isolation and characterization of mouse nasal-associated lymphoid tissue. J. Immunol. Methods **202:**123–131.
2. **Aversa, G., C. C. Chang, J. M. Carballido, B. G. Cocks, and J. E. de Vries.** 1997. Engagement of the signaling lymphocytic activation molecule (SLAM) on activated T cells results in IL-2-independent, cyclosporin A-sensitive T cell proliferation and IFN-gamma production. J. Immunol. **158:**4036–4044.
3. **Bieback, K., E. Lien, I. M. Klagge, E. Avota, J. Schneider-Schaulies, W. P. Duprex, H. Wagner, C. J. Kirschning, V. Ter Meulen, and S. Schneider-Schaulies.** 2002. Hemagglutinin protein of wild-type measles virus activates Toll-like receptor 2 signaling. J. Virol. **76:**8729–8736.
4. **Bryce, J., C. Boschi-Pinto, K. Shibuya, R. E. Black, and WHO Child Health Epidemiology Reference Group.** 2005. WHO estimates of the causes of death in children. Lancet **365:**1147–1152.
5. **Cherry, J.** 2003. Measles virus, p. 2283–2304. *In* C. J. Buck, G. Demmler, and S. Kaplan (ed.), Textbook of pediatric infectious diseases. Elsevier Health Sciences, Philadelphia, PA.
6. **Cocks, B. G., C. C. Chang, J. M. Carballido, H. Yssel, J. E. de Vries, and G. Aversa.** 1995. A novel receptor involved in T-cell activation. Nature **376:**260–263.
7. **Condack, C., J.-C. Grivel, P. Devaux, L. Margolis, and R. Cattaneo.** 2007. Measles virus vaccine attenuation: suboptimal infection of lymphatic tissue and tropism alteration. J. Infect. Dis. **196:**541–549.
8. **de Swart, R. L., M. Ludlow, L. de Witte, Y. Yanagi, G. van Amerongen, S. McQuaid, S. Yuksel, T. B. H. Geijtenbeek, W. P. Duprex, and A. D. M. E. Osterhaus.** 2007. Predominant infection of CD150+ lymphocytes and dendritic cells during measles virus infection of macaques. PLoS Pathogens **3:**e178.
9. **de Swart, R. L.** 2009. Measles studies in the macaque model. Curr. Top. Microbiol. Immunol. **330:**55–72.
10. **de Witte, L., R. D. de Vries, M. van der Vlist, S. Yuksel, M. Litjens, R. L. de Swart, and T. B. H. Geijtenbeek.** 2008. DC-SIGN and CD150 have distinct roles in transmission of measles virus from dendritic cells to T-lymphocytes. PLoS Pathog. **4:**e1000049.
11. **Dorig, R. E., A. Marcil, A. Chopra, and C. D. Richardson.** 1993. The human CD46 molecule is a receptor for measles virus (Edmonston strain). Cell **75:**295–305.
12. **Duprex, W. P., I. Duffy, S. McQuaid, L. Hamill, S. L. Cosby, M. A. Billeter, J. Schneider-Schaulies, V. ter Meulen, and B. K. Rima.** 1999. The H gene of rodent brain-adapted measles virus confers neurovirulence to the Edmonston vaccine strain. J. Virol. **73:**6916–6922.
13. **Erlenhoefer, C., W. J. Wurzer, S. Loffler, S. Schneider-Schaulies, V. ter Meulen, and J. Schneider-Schaulies.** 2001. CD150 (SLAM) is a receptor for measles virus but is not involved in viral contact-mediated proliferation inhibition. J. Virol. **75:**4499–4505.
14. **GeurtsvanKessel, C. H., M. A. M. Willart, L. S. van Rijt, F. Muskens, M. Kool, C. Baas, K. Thielemans, C. Bennett, B. E. Clausen, H. C. Hoogsteden, A. D. M. E. Osterhaus, G. F. Rimmelzwaan, and B. N. Lambrecht.** 2008. Clearance of influenza virus from the lung depends on migratory langerin+CD11b− but not plasmacytoid dendritic cells. J. Exp. Med. **205:**1621–1634.
15. **Grayson, M. H., and M. J. Holtzman.** 2007. Emerging role of dendritic cells in respiratory viral infection. J. Mol. Med. **85:**1057–1068.
16. **Griffin, D. E.** 2007. Measles virus, p. 1551–1585. *In* D. M. Knipe and P. M. Howley (ed.), Fields virology, 5th ed., vol. 1. Lippincott Williams and Wilkins, Philadelphia, PA.
17. **Hahm, B., N. Arbour, D. Naniche, D. Homann, M. Manchester, and M. B. Oldstone.** 2003. Measles virus infects and suppresses proliferation of T lymphocytes from transgenic mice bearing human signaling lymphocytic activation molecule. J. Virol. **77:**3505–3515.
18. **Hahm, B., N. Arbour, and M. B. A. Oldstone.** 2004. Measles virus interacts with human SLAM receptor on dendritic cells to cause immunosuppression. Virology **323:**292–302.
19. **Harmsen, A. G., B. A. Muggenburg, M. B. Snipes, and D. E. Bice.** 1985. The role of macrophages in particle translocation from lungs to lymph nodes. Science **230:**1277–1280.
20. **Hsu, E. C., C. Iorio, F. Sarangi, A. A. Khine, and C. D. Richardson.** 2001. CDw150(SLAM) is a receptor for a lymphotropic strain of measles virus and may account for the immunosuppressive properties of this virus. Virology **279:**9–21.
21. **Kärber, G.** 1931. Beitrag zur kollektiven Behandlung pharmakologischer Reihenversuche. Arch. Exp. Pathol. Pharmakol. **162:**480–483.
22. **Kumagai, Y., O. Takeuchi, H. Kato, H. Kumar, K. Matsui, E. Morii, K. Aozasa, T. Kawai, and S. Akira.** 2007. Alveolar macrophages are the primary interferon-alpha producer in pulmonary infection with RNA viruses. Immunity **27:**240–252.
23. **Legge, K. L., and T. J. Braciale.** 2003. Accelerated migration of respiratory dendritic cells to the regional lymph nodes is limited to the early phase of pulmonary infection. Immunity **18:**265–277.
24. **Leonard, V. H. J., P. L. Sinn, G. Hodge, T. Miest, P. Devaux, N. Oezguen, W. Braun, P. B. McCray, M. B. McChesney, and R. Cattaneo.** 2008. Measles virus blind to its epithelial cell receptor remains virulent in rhesus monkeys but cannot cross the airway epithelium and is not shed. J. Clin. Investig. **118:**2448–2458.
25. **Mavaddat, N., D. W. Mason, P. D. Atkinson, E. J. Evans, R. J. Gilbert, D. I. Stuart, J. A. Fennelly, A. N. Barclay, S. J. Davis, and M. H. Brown.** 2000. Signaling lymphocytic activation molecule (CDw150) is homophilic but self-associates with very low affinity. J. Biol. Chem. **275:**28100–28109.
26. **McChesney, M. B., C. J. Miller, P. A. Rota, Y. D. Zhu, L. Antipa, N. W. Lerche, R. Ahmed, and W. J. Bellini.** 1997. Experimental measles. I. Pathogenesis in the normal and the immunized host. Virology **233:**74–84.
27. **Minagawa, H., K. Tanaka, N. Ono, H. Tatsuo, and Y. Yanagi.** 2001. Induction of the measles virus receptor SLAM (CD150) on monocytes. J. Gen. Virol. **82:**2913–2917.
28. **Moss, W. J.** 2009. Measles control and the prospect of eradication. Curr. Top. Microbiol. Immunol. **330:**173–189.
29. **Mrkic, B., J. Pavlovic, T. Rulicke, P. Volpe, C. J. Buchholz, D. Hourcade, J. P. Atkinson, A. Aguzzi, and R. Cattaneo.** 1998. Measles virus spread and pathogenesis in genetically modified mice. J. Virol. **72:**7420–7427.
30. **Müller, U., U. Steinhoff, L. F. Reis, S. Hemmi, J. Pavlovic, R. M. Zinkernagel, and M. Aguet.** 1994. Functional role of type I and type II interferons in antiviral defense. Science **264:**1918–1921.
31. **Naniche, D., G. Varior-Krishnan, F. Cervoni, T. F. Wild, B. Rossi, C. Rabourdin-Combe, and D. Gerlier.** 1993. Human membrane cofactor protein (CD46) acts as a cellular receptor for measles virus. J. Virol. **67:**6025–6032.
32. **Navaratnarajah, C. K., V. H. J. Leonard, and R. Cattaneo.** 2009. Measles virus glycoprotein complex assembly, receptor attachment and cell entry. Curr. Top. Microbiol. Immunol. **329:**59–76.
33. **Ohno, S., N. Ono, F. Seki, M. Takeda, S. Kura, T. Tsuzuki, and Y. Yanagi.** 2007. Measles virus infection of SLAM (CD150) knockin mice reproduces tropism and immunosuppression in human infection. J. Virol. **81:**1650–1659.
34. **Ono, N., H. Tatsuo, K. Tanaka, H. Minagawa, and Y. Yanagi.** 2001. V

domain of human SLAM (CDw150) is essential for its function as a measles virus receptor. J. Virol. **75:**1594–1600.
35. **Radecke, F., P. Spielhofer, H. Schneider, K. Kaelin, M. Huber, C. Dotsch, G. Christiansen, and M. A. Billeter.** 1995. Rescue of measles viruses from cloned DNA. EMBO J. **14:**5773–5784.
36. **Roscic-Mrkic, B., R. A. Schwendener, B. Odermatt, A. Zuniga, J. Pavlovic, M. A. Billeter, and R. Cattaneo.** 2001. Roles of macrophages in measles virus infection of genetically modified mice. J. Virol. **75:**3343–3351.
37. **Sakaguchi, M., Y. Yoshikawa, K. Yamanouchi, T. Sata, K. Nagashima, and K. Takeda.** 1986. Growth of measles virus in epithelial and lymphoid tissues of cynomolgus monkeys. Microbiol. Immunol. **30:**1067–1073.
38. **Sauer, K. A., P. Scholtes, R. Karwot, and S. Finotto.** 2006. Isolation of CD4+ T cells from murine lungs: a method to analyze ongoing immune responses in the lung. Nat. Protoc. **1:**2870–2875.
39. **Schneider-Schaulies, S., and J. Schneider-Schaulies.** 2009. Measles virus-induced immunosuppression. Curr. Top. Microbiol. Immunol. **330:**243–269.
40. **Sellin, C. I., N. Davoust, V. Guillaume, D. Baas, M.-F. Belin, R. Buckland, T. F. Wild, and B. Horvat.** 2006. High pathogenicity of wild-type measles virus infection in CD150 (SLAM) transgenic mice. J. Virol. **80:**6420–6429.
41. **Sellin, C. I., and B. Horvat.** 2009. Current animal models: transgenic animal models for the study of measles pathogenesis. Curr. Top. Microbiol. Immunol. **330:**111–127.
42. **Shingai, M., N. Inoue, T. Okuno, M. Okabe, T. Akazawa, Y. Miyamoto, M. Ayata, K. Honda, M. Kurita-Taniguchi, M. Matsumoto, H. Ogura, T. Taniguchi, and T. Seya.** 2005. Wild-type measles virus infection in human CD46/CD150-transgenic mice: CD11c-positive dendritic cells establish systemic viral infection. J. Immunol. **175:**3252–3261.
43. **Sidorenko, S. P., and E. A. Clark.** 1993. Characterization of a cell surface glycoprotein IPO-3, expressed on activated human B and T lymphocytes. J. Immunol. **151:**4616–4624.
44. **Sidorenko, S. P., and E. A. Clark.** 2003. The dual-function CD150 receptor subfamily: the viral attraction. Nat. Immunol. **4:**19–24.
45. **Takeda, M., K. Takeuchi, N. Miyajima, F. Kobune, Y. Ami, N. Nagata, Y. Suzaki, Y. Nagai, and M. Tashiro.** 2000. Recovery of pathogenic measles virus from cloned cDNA. J. Virol. **74:**6643–6647.
46. **Takeuchi, K., M. Takeda, N. Miyajima, Y. Ami, N. Nagata, Y. Suzaki, J. Shahnewaz, S. Kadota, and K. Nagata.** 2005. Stringent requirement for the C protein of wild-type measles virus for growth both in vitro and in macaques. J. Virol. **79:**7838–7844.
47. **Tatsuo, H., N. Ono, K. Tanaka, and Y. Yanagi.** 2000. SLAM (CDw150) is a cellular receptor for measles virus. Nature **406:**893–897.
48. **Toth, A. M., P. Devaux, R. Cattaneo, and C. E. Samuel.** 2009. Protein kinase PKR mediates the apoptosis induction and growth restriction phenotypes of C protein-deficient measles virus. J. Virol. **83:**961–968.
49. **van oud Alblas, A. B., and R. van Furth.** 1979. Origin, kinetics, and characteristics of pulmonary macrophages in the normal steady state. J. Exp. Med. **149:**1504–1518.
50. **Veillette, A.** 2006. Immune regulation by SLAM family receptors and SAP-related adaptors. Nat. Rev. Immunol. **6:**56–66.
51. **von Messling, V., D. Milosevic, and R. Cattaneo.** 2004. Tropism illuminated: lymphocyte-based pathways blazed by lethal morbillivirus through the host immune system. Proc. Natl. Acad. Sci. U. S. A. **101:**14216–14221.
52. **von Messling, V., N. Svitek, and R. Cattaneo.** 2006. Receptor (SLAM, CD150) recognition and the V protein sustain swift lymphocyte-based invasion of mucosal tissue and lymphatic organs by a morbillivirus. J. Virol. **80:**6084–6092.
53. **Wang, N., A. Satoskar, W. Faubion, D. Howie, S. Okamoto, S. Feske, C. Gullo, K. Clarke, M. R. Sosa, A. H. Sharpe, and C. Terhorst.** 2004. The cell surface receptor SLAM controls T cell and macrophage functions. J. Exp. Med. **199:**1255–1264.
54. **Welstead, G. G., C. Iorio, R. Draker, J. Bayani, J. Squire, S. Vongpunsawad, R. Cattaneo, and C. D. Richardson.** 2005. Measles virus replication in lymphatic cells and organs of CD150 (SLAM) transgenic mice. Proc. Natl. Acad. Sci. U. S. A. **102:**16415–16420.
55. **Yanagi, Y., M. Takeda, and S. Ohno.** 2006. Measles virus: cellular receptors, tropism and pathogenesis. J. Gen. Virol. **87:**2767–2779.